STUDY THE THERMAL PERFORMANCE OF DRYING TOMATOES PROCESS USING A SOLAR ENERGY SYSTEM

/

دراسة التأثير الحراري لعملية تجفيف الطماطم باستخدام نظام الطاقة الشمسية

Ahmed M. EL-SHEIKHA[1)], Mohamed R. DARWESH[2,3)], Rashad HEGAZY[4)], Mahmoud OKASHA[*5)], Nada H. MOHAMED[1)]

[1)]Agricultural Engineering Dept., Faculty of Agriculture, Damietta University, Egypt
[2)]Agricultural Engineering Dept., Faculty of Agriculture, Tanta University, Egypt
[3)]Food Industry Technology Dept., Faculty of Technology of Industry and Energy, Samannoud Technological University, Egypt
[4)]Agricultural Engineering Department, Faculty of Agriculture, Kafrelsheikh University, Kafrelsheikh 33516, Egypt
[5)]Agricultural Engineering Research Institute (AEnRI), Agricultural Research Center (ARC), Giza 12611/ Egypt
Tel: +20-1003133841; E-mail: mahmoudokasha1988@yahoo.com
Corresponding author: Mahmoud Okasha
DOI: https://doi.org/10.35633/inmateh-73-01

Keywords: *Dryer; Solar energy; Tomato; Greenhouse*

ABSTRACT

This study developed a hybrid solar greenhouse dryer (lean-to) incorporated with a solar collector and photovoltaic (PV) system for smallholder processors of tomatoes and evaluated the thermal performance of forced convection mixed-mode solar dryer with two pretreatments of fresh tomatoes (halves and slices) with salt and sugar. Tomatoes dipped in a 40% sucrose solution for 72 hours before drying exhibited a greater initial drying rate than those treated with salt. The hourly average incident solar radiation without a reflector was 673.8 (±214.2) W/m² outside and 754.6 (±284.5) W/m² inside the lean-to solar dehydrator during operation. The incident solar radiation in the collector ranged from 390.3 to 1156.0 W/m², indicating higher levels at the tilt angle. The hourly average air temperatures outside and inside the solar dehydrator and solar collector during the experiment, respectively, were 30.7 (±2.3), 52.7 (±10.1), and 30.7 (±2.3), 79.7 (±26.9)°C for the salt treatment and 31.0 (±2.0), 55.1 (±15.3), and 31.0 (±2.0), 84.8 (±28.0)°C for the sugar treatment. Thus, the solar dehydrator and the solar collector raised the dehydrating air temperatures over the outside for the salt and sugar treatment by an average of 22.0, 49.0, 24.1, and 53.8ºC, respectively. The average hourly air-relative humidity inside the solar dehydrator was 33.5%, while outside was 47.2%. The pretreated tomatoes had an initial moisture content of 93.1% (w.b). The solar dehydrator's thermal efficiency was 72.21%, and its drying efficiency was 56.48%. Consequently, solar energy contributed 84.28 and 71.18% of the generated heating power. The solar dehydrator lost 15.72 and 28.82% of its remaining solar energy due to exhausted air. The solar dehydrator had a daily average energy of 59.375 kWh, and the heating power was 47.473 kWh during the experimental period (29 h).

الملخص

تهدف هذه الدراسة الى تطوير مجفف هجين يعمل بالطاقة الشمسية للبيوت الزجاجية مُدمج مع مجمع شمسي ونظام خلايا ضوئية لصغار مُصنعي الطماطم. كما تناولت الدراسة تقييم الأداء الحراري للمجفف الشمسي ذو الحمل الحراري الممزوج مع نوعين من المعالجة المسبقة للطماطم الطازجة (أنصاف وشرائح) باستخدام الملح والسكر. أظهرت الطماطم التي غُطست في محلول سكر بنسبة 40٪ لمدة 72 ساعة قبل التجفيف معدل تجفيف أولي أكبر من تلك التي تم معاملتها بالملح. كان متوسط الإشعاع الشمسي الساقط في الساعة بدون العاكس 673.8 (±214.2) واط/مترمربع في الخارج و754.6 (±284.5) واط/مترمربع داخل مجفف التجفيف الشمسي أثناء التشغيل. تراوح الإشعاع الشمسي الساقط على المجمع الشمسي بين 390.3 و1156.0 واط/مترمربع، مما يدل على مستويات أعلى عند زاوية الميل. كانت متوسطات درجات حرارة الهواء خارج المجفف الشمسي وداخله ومجمع الطاقة الشمسية خلال التجربة على التوالي 30.7 (±2.3)، 52.7 (±10.1)، 30.7 (±2.3) و79.7 (±26.9) درجة مئوية للمعاملة بالملح و31.0 (±2.0)، 55.1 (±15.3)، 31.0 (±2.0) و84.8 (±28.0) درجة مئوية للمعاملة بالسكر. وبالتالي، رفع المجفف الشمسي والمجمع الشمسي درجة حرارة الهواء المجفف عن الخارج لكلا من المعاملة بالملح والسكر بمعدل 22.0، 49.0، 24.1 و53.8 درجة مئوية، على التوالي. كان متوسط الرطوبة النسبية للهواء داخل المجفف الشمسي 33.5٪، بينما كانت بالخارج 47.2٪. وبلغت نسبة الرطوبة الأولية للطماطم المعالجة مسبقًا 93.1٪ (على أساس الوزن الرطب). وبلغت الكفاءة الحرارية للمجفف الشمسي 72.21٪، وكانت كفاءة التجفيف 56.48٪. وبالتالي، ساهمت الطاقة الشمسية بنسبة 84.28 و71.18٪ من طاقة التسخين المتولدة. وفقد المجفف الشمسي 15.72 و28.82٪ من طاقته الشمسية المتبقية بسبب الهواء الخارج. وبلغ متوسط الطاقة اليومية للمجفف الشمسي 59.375 كيلووات ساعة، بينما كانت قدرة التسخين 47.473 كيلووات ساعة خلال الفترة التجريبية (29 ساعة).

INTRODUCTION

Tomato (*Lycopersicon esculentum* Mill.) is a commonly cultivated vegetable worldwide, boasting a productivity of approximately 182,301,395 tons from an area of 4,848,384 ha. China, the USA, Turkey, India, and Egypt are leading global tomato producers.

Egypt produced 6,275,443 tons of tomatoes in 2022 (*FAO, 2022*). After harvest, the drying process is implemented by many local processors as an effective means to extend the shelf life of tomato crops (*Li, 2021*). Solar energy is a well-established and renewable source, especially for low-temperature heating. Solar drying is the most optimal solution to overcome artificial mechanical and natural sun drying drawbacks. Moreover, adopting solar energy for crop drying offers both environmental benefits and economic viability in developing countries. Providing energy for agricultural applications is contingent upon advancing solar energy systems with optimal thermal performance, exceptional reliability, and competitive economic features. This advancement must attain a stage where optimal thermal performance and reliability can be attained for a wide range of solar energy applications. For solar energy to be economically viable, solar energy systems must exhibit high annual utilization, extended lifespan, and meticulous design tailored to the specific application and location, thus enabling a realistic evaluation of solar energy as a feasible alternative energy source. Consequently, solar energy is a viable heat source for drying various crops. Because of the uncertain rise in fossil fuel prices and the potential depletion, it has received significant attention in recent years (*Abdellatif et al., 2015; Ramos et al., 2015*). Fruits and vegetables, including potato slices, red peppers, cherry tomatoes, banana slices, and tomatoes, have been subjected to solar drying techniques. There have been few studies conducted on the solar drying of cherry tomatoes. Several studies were conducted to investigate the thermal and mass transfer balance in hybrid solar dryers and the effectiveness of solar greenhouse dryers (*Azam et al., 2020*). *Patil and Gawande* (*2016*) reviewed various techniques employed in greenhouse dryers and solar tunnels, focusing on forced and natural convection methods. Using tunnels and greenhouses for solar drying proves to be highly suitable for rural areas. Using these dryers leads to substantial fuel savings and enhances the product's quality regarding color, taste, and aroma. The enhancement of dried agricultural products' quality is of utmost importance, and this can be accomplished by implementing pretreatment methods that ensure product preservation and enhance their visual appeal. Osmosis is a convenient and effective method for pretreating fruit before drying. Immersing products in the solution reduces costs by removing water. Osmosis pretreatment might enhance the drying rate of cashew apples by impacting both their quality and drying kinetics compared to fruits that have not undergone pretreatment (*Shahi et al., 2016*). The dryer and collector had average energy efficiencies of 50.5%, and 34.98%, respectively. *Tiwari and Tiwari* (*2016*) studied the exergoeconomic of PV-thermal mixed-mode greenhouse solar dryer. *Lakshmi et al.* (*2019*) investigated stevia leaf drying in a mixed-mode forced convection solar dryer. The dryer's overall efficiency was approximately 33.5%. The dryer's payback duration is approximately 0.65 years. A hybrid solar drying system, including a greenhouse dryer, a flat plate solar collector (FPSC), and a PV system, was investigated in some literature using forced thermal convection drying mode.

Thus, this study involves developing a solar greenhouse dryer for post-harvest tomato drying and evaluating the thermal performance of hybrid forced convection mixed-mode greenhouse dryers, integrating tomato load, solar air collectors, and PV system operation.

MATERIALS AND METHODS

The trials were performed at the Faculty of Agriculture, University of Damietta (31°39′07.05″ E, longitude; 31°25′38.24″ N, latitude) from August 20th, 2022, to August 26th, 2022.

Description of the solar dehydrator (lean-to)

It comprises space heating for pre-heating the drying air, a drying chamber, and a reflector for increasing the solar radiation intensity. The structural frame comprises 12.7 mm diameter hot-dipped galvanized pipes with anti-corrosion qualities. The structural frame consists of beams, posts, and rafters that can be assembled on the spot by joining parts, bolts, and nuts with no welding points to secure optimal anti-corrosion performance. It was 2.0 m long, 1.0 m wide, 0.96 m high vertical back wall (reflector), 40 cm high vertical front wall, 1.15 m rafter length. The rafter tilt angle is 17.97º for August. The net dehydration surface area is 2.0 m^2, and the net air volume is 1.36 m^3. The drying tray is a 2.0 m long and 1.0 m wide galvanized wire mesh with a 2.0 m^2 surface area. Below the drying tray lies an air chamber comprising two layers of a 2.0 mm thick firm galvanized sheet. These layers are separated by a 2.5 cm space and filled with loosely packed rock-wool insulation to lessen heat energy gain or loss. It was 2.0 m long, 1.0 m wide, 40 cm deep, 2.0 m^2 surface area, and 0.8 m^3 space volume. To circulate the dehydrated air through the solar dehydrator, an electric forced air fan with a power of 38 W, a speed of 2000 rpm, and operating at a current of 220 V is positioned at the center of the eastern side (lateral section) of an air chamber. This fan is connected to an air duct with a diameter of 12 cm. On the opposite side, the solar dehydrator's gable incorporates a circular opening with a 12 cm diameter (inlet for drying air) at its center.

This configuration ensures that air enters the upper section's solar dehydrators and descends through the drying tomatoes before being expelled from the dehydrator. The solar dehydrator is located 10 cm above the floor level using four metallic legs over a cubic concrete block (20×20 cm), as shown in Fig. 1.

The dehydration chamber's upper surface was covered by a perforated galvanized steel sheet, and the other sides were covered with sold galvanized steel sheets. The solar dehydrator is equipped with a transparent polycarbonate sheet that is 2.0 mm thick, providing UV protection and allowing for high radiation transmission to optimize the dehydrator's solar radiation. A 2.0 mm thick sheet of nickel chrome was applied to the vertical back wall as a solar reflector. The solar dehydrator was in an East-West orientation.

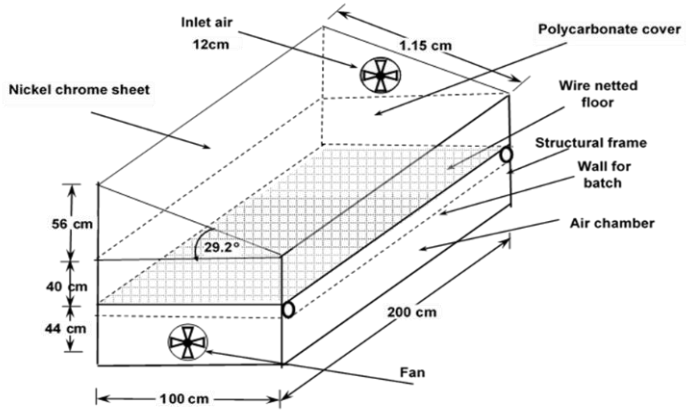

Fig. 1 – Simplified scheme and picture of solar dehydrator (lean-to architectural form)

Flat plate air solar collector

It comprises space heating for pre-heating the air, a wooden box, and an absorber plate for increasing the intensity of solar radiation. It was inclined with 30° and supplied the lean-to solar dryer with auxiliary heat. The structural frame was made from wood with a 2.0 m^2 surface area (2.0 m long, 1.0 m wide), 0.15 m depth, and 0.3 m^3 space volume. It had 2.5 cm rock-wool insulation to lessen heat gain or loss. It has a black-painted aluminum corrugated sheet of 0.002 m thick, and the thermal conductivity coefficient was 204 W/m.°C, which was utilized to absorb thermal solar radiation and used it to heat the air, which moves up toward the solar dryer. A 0.10 m fiberglass insulation layer was installed to insulate the absorber plate from the backside to minimize heat energy gain or loss. The upper surface of the solar collector was protected by a polycarbonate sheet measuring 0.002 m, maintaining a gap of approximately 0.10 m between the absorber sheet and polycarbonate to facilitate airflow. The upward movement of hot air from the collector toward the lean-to solar dryer occurs through an insulated tube measuring 0.15 m in diameter, as depicted in Fig. 2.

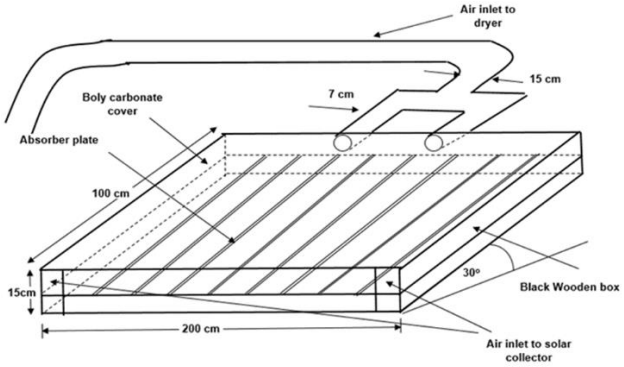

Fig. 2 – Simplified scheme of flat plate air solar collector (architectural form)

Solar photovoltaic cell (PV) panels

The PV system included a 385 W ASEM PV panel, a charge controller with 12 V/24 V capabilities and load current up to 20 A, and a 12 V battery with a rated current of 17 A h). Inverter (Yumatsu JAPAN 220V 50Hz/60Hz Power capacity: 2000VA). This was used to convert the current to DC, which comes from the PV panel and is integrated into the battery. The PV panel's inclination was set to 30° in a southerly direction. The PV system was used to power a DC fan, which helped optimize the drying process, as revealed in Fig. 3.

Fig. 3 – Tomatoes spread under natural sun drying

Experimental parameters of PV-solar collector incorporated with greenhouse dryer

An evaluation was performed to measure the performance of the greenhouse dryer when used outdoors, specifically for drying tomatoes. The initial trials were performed at varying airflow rates of 2.10, 3.12, and 4.18 m^3/min, utilizing the DC speed controller to regulate the DC fan's flow rate. The optimal airflow rate of 3.12 m^3/min was elected for drying tomatoes. Fresh tomatoes were purchased from the local market in 2022. Before the drying process, the selected fresh tomatoes were subjected to a cleaning and pre-conditioning procedure, which involved the removal of foreign impurities and immatureness. As a result, a homogeneous size of tomatoes unaffected by bacteria and fungi was chosen for the experimental investigation. These tomatoes were carefully graded by hand, with a preference for smaller sizes (0.020-0.035 m diameter). After washing, the tomatoes were divided into two groups of equal weight (7.0 kg each). Fresh tomatoes were halved and sliced, then osmotically treated with sugar. They were compared to halved and sliced tomatoes, treated with salt, and dried in the greenhouse dryer. The fruits treated osmotically with sugar are cut into halves and slices and dipped in a 40% sucrose solution for 72 h (10.5-liter water/ 2.8 kg sugar/ 7kg of tomatoes). The samples were stored at 5°C before beginning the experiments and then allowed to reach room temperature.

Measurements

The ambient weather and various parameters of the greenhouse dryer (GD) were measured using instruments, including a meteorological weather station (Vantage Pro 2, Devise, USA). This allowed for accurately evaluating the macroclimatic conditions surrounding the developed drying system. These measurements comprise various weather factors, including solar radiation intensity on a horizontal plane, dry-bulb air temperature, air relative humidity, and wind speed. The weather station is beside the solar dehydrator (about five meters away). The collected data were stored in a computer file for data acquisition. The speed of dehydrated air was measured thrice daily at the drying air inlet and outlet locations throughout the experimental duration. This was conducted using a vane LCD Digital Anemometer (Montreal, Canada). Solar radiation intensity was measured using disk-solarimeters (TENMARS TM-207, Taiwan). They were placed horizontally with the dryer and were inclined toward the PV module and the solar collector. Temperature and relative humidity were measured by a weather anemometer sensor (Pasport, 1000 series, USA). Measurements of the relative humidity in the ambient air and inside the dryer were conducted using the Amprobe THWD-5. The dryer's airflow rate and wind speed were measured using an airflow meter/Hotwire anemometer. The moisture content of tomatoes was determined using an electric oven dryer set at a temperature of 70 ± 1°C (*ASAE 1991*). The initial, final, and instantaneous moisture contents were calculated based on dry basis according to *Mumba (1996*), as follows in Eqs. 1–3:

$$M_0 = \frac{W_0 - W_d}{W_d} \quad (1)$$

$$M_f = \frac{W_{wet} - W_d}{W_d} \quad (2)$$

$$M_t = \left[\frac{(M_0 + 1)W_0}{W_t} - 1\right] = \frac{(W_t - W_d)}{W_d} \quad (3)$$

where:

M_0 denotes the initial moisture content [%], W_0 represents the initial weight of sample [kg], W_d represents the weight of dry matter [kg], M_f implies the final moisture content [%], M_t implies the instantaneous moisture content [%], and W_t represents the weight of sample at time (t) [kg].

Thermal energy balance analysis

An energy analysis of tomato drying with a PV solar collector integrated with a lean-to solar dryer is presented in this study. The steady-state energy equations are used to optimize tomato drying conditions (*Hepbasli, 2008*).

The net energy balance between the inlet and outlet can be represented by Eq. 4:

$$\sum E_{in} = \sum E_{out} \tag{4}$$

where E_{in} denotes the net energy input, [W], E_{out} represents the net energy outlet, [W].

Solar collector's thermal balance

The solar collector's thermal balance was determined as follows in Eqs. 5–7:

$$E_{in,coll} = E_{out,coll} \tag{5}$$

$$E_{in,coll} = (E_{out,coll} + E_{heat\ transfered} + E_{infiltration}) \tag{6}$$

$$E_{u,coll} = E_{in,coll} - (E_{heat\ transfered} + E_{infiltration}) \tag{7}$$

The energy input and heat gain of the solar collector are computed by *Duffie and Beckman* (*2013*); *Usub et al.* (*2008*), as follows in Eqs. 8–10:

$$E_{in,coll} = E_{solar,coll} = A_{coll} \int_0^t I_{coll} \tag{8}$$

$$E_{u,coll} = m_a \times C_{p,a}(T_{a,in} - T_{a,out}) \tag{9}$$

$$m_a = \rho_a \times V_a = \rho_a \times u_a \times A_{call} \tag{10}$$

where m_a denotes the air mass flow rate, [kg/s]; A_{coll} represents the collector area [m^2], ua implies air speed, [m/s]; and ρ_a stands for the air density, [kg/m^3].

Hence, collector efficiency (η_{coll}) is calculated as follows in Eqs. 11–13:

$$\eta_{coll} = \frac{E_{u,coll}}{E_{in,coll}} \tag{11}$$

$$E_{loss} = E_{heat\ transfer} + E_{infiltration} \tag{12}$$

$$E_{heat\ transfer} = E_{wall} + E_{ground} + E_{loss,tube} \tag{13}$$

Heat losses from solar collector surfaces can be determined according to *Sahin and Sumnu* (*2005*), as follows in Eqs. 14 and 15:

$$E_{heat\ transfer(surfaces)} = U_{coll,surf} \times A_{coll,surf} \times dT \tag{14}$$

$$U_{coll,surf} = \frac{1}{\left(\frac{1}{h_{conv,abs-g}} + \frac{X_1}{h_{rad,abs-g}} + \frac{1}{h_{rad,g-amb}} + \frac{X_1}{h_{conv,g-amb}}\right)} \tag{15}$$

Where:

$U_{coll,surf}$ denotes the overall heat transfer coefficient for the solar collector surfaces [W/m^2.K],

$A_{coll,surf}$ denotes the solar collector's area [m^2], and dT refers to the temperature difference [K].

Heat losses from collector walls and ground to air

The convective and conductive resistances of the overall heat transfer coefficient were determined as follows in Eq. 16:

$$U_{coll,wg} = \frac{1}{\left(\frac{1}{h_i} + \frac{x_1}{k_1} + \frac{x_2}{k_2} + \frac{x_3}{k_3} + \frac{1}{h_o}\right)} \tag{16}$$

where h_i and h_o represent the heat transfer coefficients for internal and external surfaces [W/m^2.K], respectively, x_i is the layer's thickness [m], k_i is the layer's thermal conductivity [W/m.K].

The solar collector's walls and ground heat losses can be determined using Eq. 17:

$$E_{heat\ transfer(wall,ground)} = U_{coll,wg} \times A_{coll,wg} \times dT \tag{17}$$

where $U_{coll,wg}$ refers to the overall heat transfer coefficient [W/m^2.K], $A_{coll,wg}$ stands for the solar collector's area of walls and ground [m^2], and dT denotes the temperature difference [K].

Heat transfer by convection from the collector

The convective heat transfer coefficient caused by wind is calculated based on *Duffie and Beckmen* (*2013*), as follows in Eq. 18:

$$h_{g-amb,coll} = 2.8 + (3.0 \times W_s) \quad (18)$$

The convective heat transfer coefficient for air over the absorber surface can be calculated by determining the Reynolds Number (Re) and Nusselt number (Nu) *Bergman et al.* (*2011*), as follows in Eqs. 19–21:

$$Re = \frac{u_{a,coll} \times \rho_a \times D_{h,coll}}{v_a} \quad (19)$$

$$Nu = \frac{h_{conv,abs-a} \times D_h}{k_a} = 0.0158Re^{0.8} \quad (20)$$

$$h_{conv,abs-a} = \frac{k_a \times Nu}{D_{h,coll}} \left(\frac{W}{m^2 \times ℃}\right) \quad (21)$$

where $D_{h,coll}$ stands for the air passes hydraulic width (m), and is determined according to *Cengel et al.* (*2003*), as follows in Eq. 22:

$$D_{h,coll} = \frac{4(D \times H)}{2(D + H)} \quad (22)$$

where D_{coll} and H_{coll} represent the actual width and height of the air passes [1 m and 0.08 m, respectively], Dh is the air pass width [m], v is the air viscosity [m²/s], $Tabs$ is the absorber temperature [65℃ = 338K], and $Tamb$ is the surrounding temperature [31℃ = 304K]. Thus, $h_{conv,abs-a}$ = 1.746 W/m².K; and heat loss below the absorber is obtained as shown in Eq. 23:

$$E_{conv,(abs-a)} = A_{abs} \times h_{conv,abs-a} \times (T_{abs} - T_{amb}) \quad (23)$$

where A_{abs} represents the contact area between the absorber and the air within the collector [m²].

Collector's radiation heat transfer ($E_{rad,coll}$)

The radiation heat transfer coefficients can be determined by employing Eqs. 24 and 25 given by *Duffie and Beckmen* (*2013*) for the interactions between the sky and the collector glass cover and between the absorber and collector glass cover.

$$h_{rad,g-s} = \varepsilon_g \times \sigma \times (T_g^2 + T_s^2) \times (T_g + T_s) \quad (24)$$

$$h_{rad,abs-g} = \frac{\sigma \times \left(T_{abs}^2 + T_g^2\right) \times \left(T_{abs} + T_g\right)}{\frac{1}{\varepsilon_{abs}} + \frac{1}{\varepsilon_g} - 1} \quad (25)$$

where ε_{abs} represent the emissivity of the absorber surface [assumed 0.98], ε_g represents the emissivity of the glass surface [assumed 0.92], and s represents the Stefan-Boltzmann constant [5.67×108 W/m².K⁴]. The sky temperature (Ts) is calculated according to *Duffie and Beckmen (2013)*, as in Eq. 26.

$$T_s = 0.0552 \times (T_{amb})^{1.5} \quad (26)$$

where Ts and T_{amb} are expressed in Kelvin. The losses caused by radiation and convection from the insulation layer surrounding the sides and bottom of the solar collector were determined using Eq. 17.

Tube heat losses between the collector and greenhouse dryer

The connection tube, which links the collector and greenhouse dryer, was constructed using tin and insulated with fiberglass. Therefore, the total heat transfer coefficient for the tube (U_{tube}) is determined in Eq.27:

$$U_{tube} = \frac{1}{\left(\frac{1}{r_i h_i} + \frac{x_1}{k_1} + \frac{x_2}{k_2} + \frac{1}{r_o h_o}\right)} \quad (27)$$

where r_i and r_o represent the inner and outer layer radius, [m], in order. The heat losses from the connection tube ($E_{loss,tube}$) are expressed as follows in Eq. 28:

$$E_{loss,tube} = 2\pi L \times \frac{(T_i - T_o)}{\left(\frac{1}{r_i h_i} + \frac{\ln\left(\frac{r_2}{r_1}\right)}{k} + \frac{1}{r_o h_o}\right)} \quad (28)$$

where h_o = h_d stands for the conductive heat-transfer coefficient across the insulation, [W/m^2.^{o}C] and is determined as follows in Eq. 29:

$$h_d = \frac{K_{gf}}{d_i} \quad (29)$$

where K_{gf} stands for thermal conductivity for fiberglass 0.043 [W/m.^{o}C], and d_i denotes the average insulation thickness [0.05 m].

Greenhouse dryer's thermal balance

In order to estimate the thermal performance of the tomato dryer, the GD underwent experiments in which the heat balance and theoretical analysis were applied according to *Dewanto et al. (2002); Lewicki (1998*), as follows in Eq. 30:

$$E_{in,dryer} = \left(E_{net,coll} + E_{sol,dryer}\right) \quad (30)$$

$$E_{out,dryer} = \left(E_{evap} + E_{loss}\right)$$

$$E_{net,dryer} = E_{sol,dryer} + E_{net,coll} - \left(E_{evap} + E_{loss}\right)$$

Heat gain to the greenhouse dryer

Solar energy in the greenhouse dryer can be determined by considering the solar radiation and surface area, as follows in Eq. 31:

$$E_{sol,dryer} = I_{dryer} \times A_{dryer} \quad (31)$$

where I_{dryer} represents the horizontal insolation on the GD, [W/m^2], and A_{dryer} denotes the area of the GD, [m^2]. The collector transfers heat to the GD, resulting in a useful heat gain as expressed in Eq. 32:

$$E_{net,coll} = E_{u,coll} \times E_{loss,tube} \quad (32)$$

Heat evaporated from the greenhouse dryer

The overall thermal energy required for evaporation (E_{evap}) comprises two components: sensible heat (E_{sens}), which raises the temperature of tomatoes to the desired level, and latent heat energy (E_{latent}), which vaporizes water from tomatoes, as follows in Eq. 33:

$$E_{evap} = E_{sens} \times E_{latent} \quad (33)$$

The estimation of the sensible heat required to increase the temperature of tomato (E_{sens}) can be determined as follows in Eq. 34:

$$E_{sens} = m_t \times C_{p,t} \times \Delta T_t = \rho_t \times V_t \times C_{p,t} \times \Delta T_t \quad (34)$$

where m_t represents fresh tomatoes rate, [kg/s], $c_{p,t}$ stands for tomato's specific heat, [4.08 kJ/kg.^{o}C], ρ_t denotes tomato's density [672.78 kg/m^3], $T_{t,in}$ refers to the tomato's inlet temperature to the dryer, [^{o}C], and $T_{t,out}$ denotes the tomato's outlet temperature from the dryer, [^{o}C].

The latent heat required for vaporizing water from tomatoes can be determined as follows in Eq. 35:

$$E_{latent} = mw \times \lambda w \quad (35)$$

where mw represents the water removal rate from tomatoes, [kg/s], and λw denotes the latent heat of water vaporization, [2300 kJ/kg].

Hence, the dryer efficiency (η_{dryer}) is determined as follows in Eq. 36:

$$\eta_{dryer} = \frac{E_{evap}}{E_{in,dryer}} \quad (36)$$

Heat losses from the greenhouse dryer via convection and radiation

By convection

The convection heat loss coefficient from the greenhouse dryer ($h_{conv,a,dryer}$) was determined using Eqs.19–22.

By radiation

The radiation heat transfer coefficient between the greenhouse covers and the sky and between the cover and the tomatoes was determined using Eqs. 24 and 25.

Thermal radiation losses can be attributed to the surfaces of the dryer cover and the dried product. The losses of radiant heat were minimal because of the low temperatures of the surface. The heat losses by radiation from the cover surface ($E_{rad,f}$) were calculated as follows in Eq. 37:

$$E_{rad,f} = A_f \times \varepsilon_f \times F_{c-d} \times \delta = \left[\left(T_{f,out}\right)^4 - \left(T_{a,out}\right)^4\right] \quad (37)$$

where ε_f refers to the surface emissivity [assumed 0.93 for the cover], and $F_{c\text{-}d}$ denotes the dryer wall's cover surface (*Bergman et al., 2011*).

Fan's heat losses in the greenhouse dryer

In the forced convection greenhouse dryer system, the heat losses through the transparent cover are significantly lower than the direct heat loss through the exhaust vent (*Mohsenin, 2020*).

Thermal balance for PV panel

$$E_{net,pv} = E_{gain} - E_{loss} \quad (38)$$

$$E_{loss} = E_{operating} - E_{infiltration} \quad (39)$$

The photovoltaic efficiency (η_{PV}) and the solar system's overall efficiency ($\eta_{overall}$) were calculated according to *Eltawil et al.* (*2018*), as follows in Eqs. 40 and 41:

$$\eta_{PV} = \frac{E_{out,PV}}{E_{in,PV}} = \frac{V_{max,PV} \times I_{max,PV}}{Ins_{PV} \times A_{PV}} \times 100 \quad (40)$$

$$\eta_{overall} = \frac{E_{out,dryer}}{E_{in,coll} + E_{in,dryer} + E_{in,fan}} \times 100 \quad (41)$$

where: η_{PV} represents photovoltaic efficiency [%], $V_{max,PV}$ refers to the maximum PV voltage for power [V], $I_{max,PV}$ refers to the maximum PV current for power [A], Ins_{PV} denotes the insolation in the same plane of PV module [W/m^2], A_{PV}denotes the area of solar module [m^2]**,** $\eta_{overall}$ implies the solar system's overall efficiency [%], $E_{out,dryer}$ implies the dryer output, $E_{in,coll}$ denotes the insolation input on the collector, $E_{in,dryer}$ represents the incident solar energy on the dryer, and $E_{in,fan}$ refers to the DC fan energy consumption.

RESULTS AND DISCUSSION

Intensity of incident solar radiation

The dehydration of tomatoes was performed utilizing the developed drying system that was incorporated with the flat plate air solar collector (FPASC) and operated using a solar PV system. The dehydration process of tomatoes included 72 hours of bright sunshine, with 25 hours for salt pretreatment and 29 hours for sugar pretreatment in the lean-to solar dehydrator. These measurements were recorded and utilized in the dehydration process. The experiment involved measuring and monitoring the intensity of solar radiation on horizontal (I_{ho} = I_{dryer}) and inclined ($I_{inclined}$ = $I_{collector}$ = I_{PV}) surfaces. The results are summarized and presented in Table 1.

Table 1

Hourly average incident solar radiation measured and recorded outside (R_o), inside the solar dehydrator (R_i) and inclined solar collector, PV panels during the experiment, and the maximum and minimum values

Date		R_o, W/m^2	Lean-to			Solar collector = PV panels
			R_i Reflected, W/m^2	R_i Horizontal, W/m^2	R_i Total, W/m^2	R_i Inclined, W/m^2
20/08/2022	Max.	633.0	87.7	519.6	607.3	1120
	Min.	266.8	36.8	190.3	227.1	540.0
	Mean	455.6	58.0	355.2	413.2	897.8
	SD	±183.3	±26.5	±164.7	±190.2	±220.3
21/08/2022	Max.	928.3	213.2	882.4	1091.9	1131.0
	Min.	275.5	69.0	285.4	285.3	399.0
	Mean	596.0	155.4	528.6	684.0	878.6
	SD	±210.2	±56.1	±220.4	±257.2	±239.3
22/08/2022	Max.	932.5	242.0	885.5	1127.5	1186.0
	Min.	301.2	59.5	238.3	297.8	430.0
	Mean	702.3	178.5	625.2	803.7	839.1
	SD	±227.1	±64.7	±232.8	±295.1	±254.6
Average	Max.	831.3	180.9	762.5	942.2	1145.7
	Min.	281.2	55.1	238.0	270.0	456.3
	Mean	584.6	130.6	503.0	633.6	871.8
	SD	±196.8	±49.1	±206.0	±247.5	±238.1

Date		R_o, W/m²	Lean-to			Solar collector = PV panels
			R_i Reflected, W/m²	R_i Horizontal, W/m²	R_i Total, W/m²	R_i Inclined, W/m²
23/08/2022	Max.	943.4	266.5	887.6	1154.1	1214.0
	Min.	441.3	59.4	248.3	307.7	353.0
	Mean	737.3	187.8	622.8	822.8	840.2
	SD	±170.4	±74.8	±217.7	±289.1	±275.7
24/08/2022	Max.	964.8	277.2	915.8	1193.0	1135.0
	Min.	309.0	66.5	256.7	323.2	320.0
	Mean	696.7	199.9	622.9	810.6	807.1
	SD	±209.1	±68.0	±214.8	±276.9	±290.8
25/08/2022	Max.	1033.3	182.0	1045.1	1227.1	1092
	Min.	329.3	91.0	225.0	316.0	341.0
	Mean	701.9	140.8	680.2	821.0	862.2
	SD	±244.2	±34.4	±282.0	±316.4	±236.7
26/08/2022	Max.	953.9	178.0	1011.6	1189.6	1224.0
	Min.	86.9	84.3	157.0	241.3	420.0
	Mean	707.9	134.6	642.2	776.8	864.6
	SD	±298.8	±25.5	±307.7	±333.3	±260.6
Average	Max.	973.9	225.9	965.0	1191.0	1166.3
	Min.	291.6	75.3	221.8	297.1	358.5
	Mean	711.0	165.8	642.0	807.8	843.5
	SD	±54.5	±59.1	±255.6	±304.0	±266.0

The incident total solar radiation inside the lean-to solar dehydrator comprised transmitted and reflected solar radiation for salt and sugar pretreatment ranged between 270.0, 942.2 W/m² and 297.1, 1191.0 W/m². The average hourly incident solar radiation outside and inside that dehydrator for salt and sugar pretreatment, without reflector was 584.6 (±196.8), 633.6 (±247.5) W/m², and 711.0 (±54.5), 807.8 (±304.0) W/m², respectively, which realized the polycarbonate cover had an average transmittance of 87.35% (±9.6) per hour. The solar radiation inside the lean-to solar dehydrator changed hourly because of the polycarbonate cover's transmittance, which is influenced by the solar incident angle. The incident total solar radiation inside the solar collector for salt and sugar pretreatment, respectively, ranged between 456.3, 1145.7 W/m² and 358.5, 1166.3 W/m², and the tilt angle recorded higher insolation than on the horizontal level. The variation in average insolation and wind speed is depicted in Fig. 4.

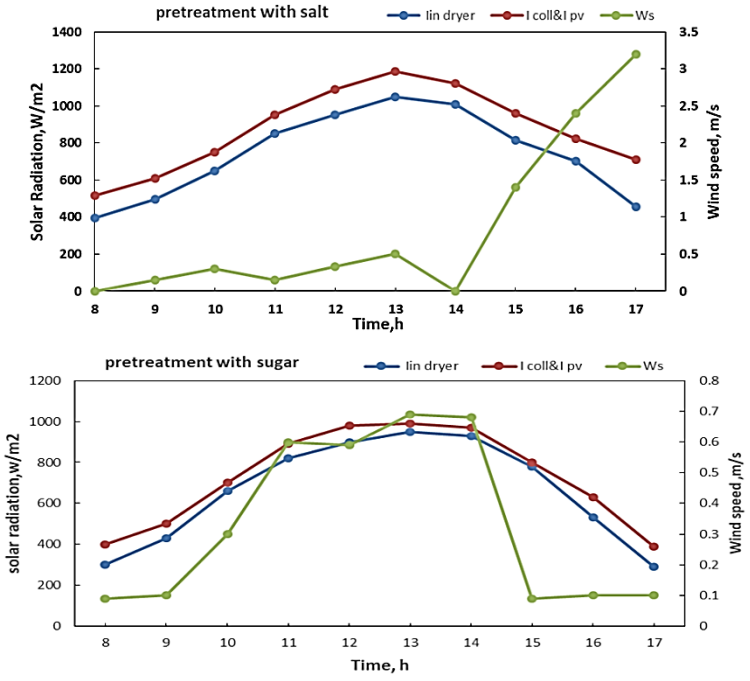

Fig. 4 – The drying system's average insolation and wind speed variation

The influence of the polycarbonate cover on the solar dehydrator was examined by plotting the incident solar radiation inside and outside the dehydrator, as shown in Figs. 5 and 6. The regression equations provided the best-fit correlations between incident solar radiation inside and outside for the solar dehydrator and solar collector, as follows in Eqs. 42, and 43:

$$R_i(lean - to) = 1.2080\ (R_o) \quad (42)$$

$$R_i(solar\ collector) = 1.3348\ (R_o) \quad (43)$$

The regression analysis revealed correlation coefficients of 0.9865 and 0.9462 between incident solar radiation inside and outside the solar dehydrator and solar collector, respectively (P > 0.001). The regression equation showed that each equation's slope almost equals the effective transmittance of the solar dehydrator cover (polycarbonate sheet). Regression analysis also showed that 10.47% and 9.49% of the outside incident solar radiation were reflected into the surrounding space of the solar dehydrator and solar collector, respectively.

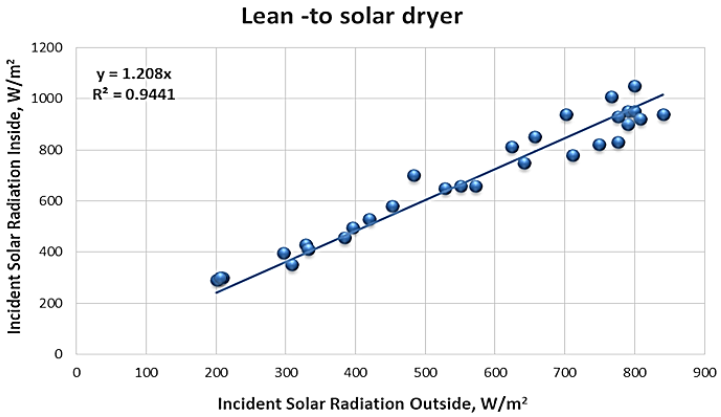

Fig. 5 – Incident solar radiation inside and outside the lean-to solar dehydrator

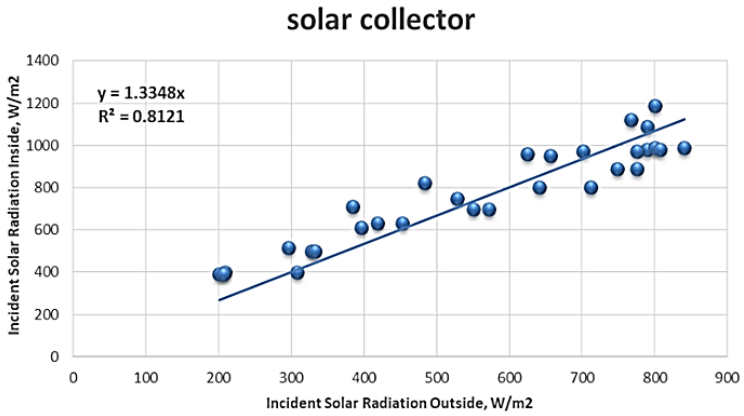

Fig. 6 – Incident solar radiation on and outside the solar collector

The relation between reflected solar radiation and incident solar radiation inside the solar dehydrator was investigated. The data regarding reflected solar radiation during the experiment were utilized to establish the correlation with incident solar radiation within the lean-to solar dehydrator (Fig. 7). The regression analysis showed a linear correlation between these two parameters, resulting in the best fit. The regression analysis also unveiled a high-significance relationship (r = 0.7584; P > 0.001). The equation used for regression analysis to find the optimal fit under certain experimental conditions is as follows in Eq. 44:

$$R_r = 0.1604(R_i) \quad (44)$$

Regression analysis also showed that the total reflected radiation from the vertical back wall almost represented 16.04% of the total incident solar radiation inside the lean-to solar dehydrator. Therefore, the reflector increased the total incident solar radiation inside the solar dehydrator over the outside incident solar radiation. Due to the lower values of solar altitude angles and higher values of solar azimuth angles and solar incident angles in the early morning and late afternoon, there was scattering in the data measured at those times.

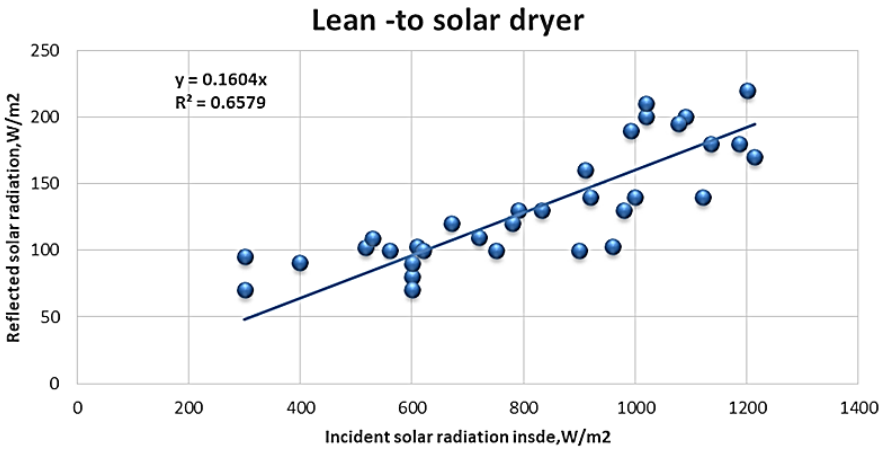

Fig. 7 – Reflected solar radiation against incident solar radiation inside the lean-to solar dehydrator during the experiment

Dehydrating-air-temperature

Average hourly air temperatures outside and inside the solar dehydrator and solar collector during the experiment, respectively, were 30.7 (±2.3), 52.7 (±10.1), and 30.7 (±2.3), 79.7 (±26.9) for the salt treatment and 31.0 (±2.0), 55.1 (±15.3), and 31.0 (±2.0), 84.8 (±28.0) for the sugar treatment. Thus, the solar dehydrator and the solar collector increased the dehydrating air temperatures over the outside for the salt and sugar treatment by an average of 22.0, 49.0ºC, and 24.1, 53.8ºC, respectively. Consequently, the increasing percentages in dehydration-air temperatures for the solar dehydrator system were 77.90%, 145.80%, 80.80%, and 180.30%, respectively.

Dehydrating-air-relative-humidity

During the dehydration process of tomatoes, the average hourly relative humidity inside the collector (RH1) and inside the solar dehydrator (RH2) was 33.5% (±7.7) and 29.1% (±7.4), respectively. The relative humidity of the outside air in salt pretreatment was 45.7% (±7.6). Regarding the sugar treatment, the average hourly relative humidity inside the solar collector (RH1) and the solar dehydrator (RH2) was measured to be 35.9% (±5.9) and 32.2% (±5.5), respectively.

Meanwhile, the relative humidity of the outside air was found to be 47.2% (±6.9). As a result, the solar collector reduced the relative humidity of the dehydrating air by 27.5% and 28.0% for the salt and sugar pretreatments, respectively, compared to the outside air relative humidity. Furthermore, the solar dehydrator effectively lowered the air-relative humidity for salt and sugar pretreatments by 4.3% and 5.7%, respectively. Fig. 8 illustrates the drying system's average temperatures and relative humidity variations. The recorded drying temperatures inside the dryer exceeded the surrounding temperature (Tout side). Simultaneously, the relative humidity level inside the GD (RH_{in}) was less than the outside (RH_{out})

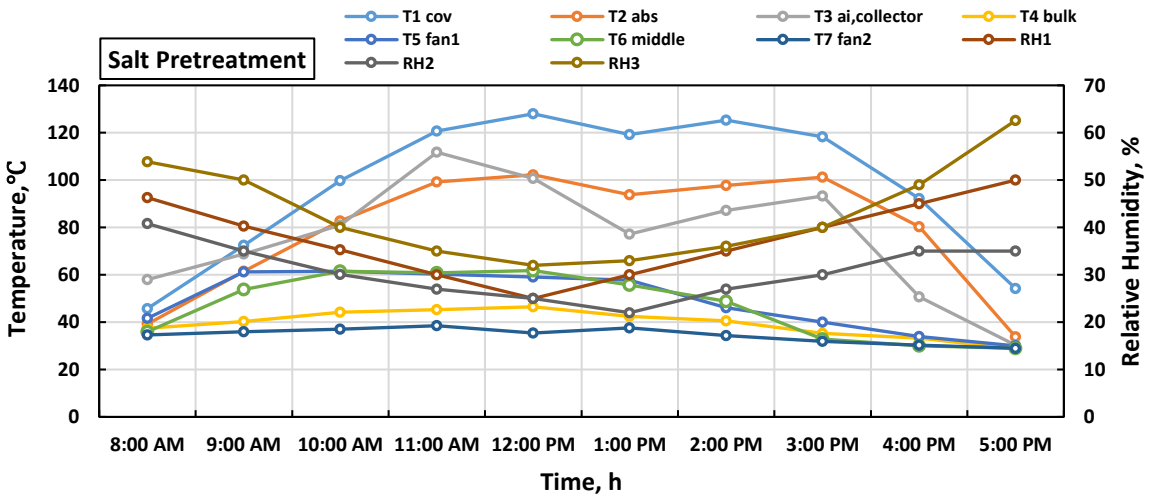

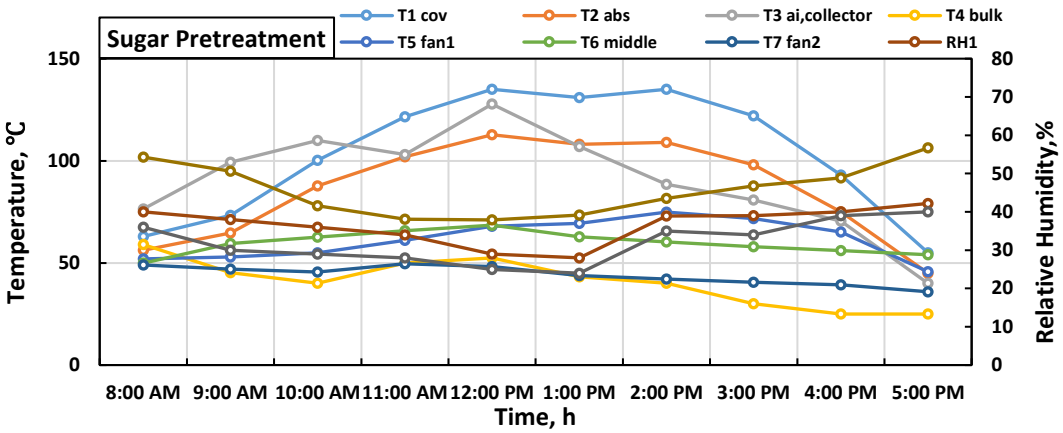

Fig. 8 – Variation of temperature and air relative humidity for salt and sugar pretreatments

Moisture content

Fig. 9 presents the moisture content variations of tomatoes at different times of the day for two treatments applied in the drying process. Increasing the duration of the drying process resulted in a decrease in the tomato's moisture content. The data concluded that the drying process of various tomato treatments follows a consistent drying rate and then transitions to a declining one. The tomatoes' moisture contents (w.b.), which dried inside the dryer for two treatments (salt and sugar) were 93.1% (10.20%) and 95.1% (11.30%), respectively. Moisture absorption during tomato pretreatment affects initial moisture content. For salt treatment, the dried tomatoes achieved equilibrium moisture content in the dryer after 20 and 25 hours for slices and halves, respectively. For sugar treatment, equilibrium moisture content was achieved by the dried tomatoes in the dryer after 23 and 29 hours for slices and halves, respectively.

To assess the impact of solar energy on heating power, the recorded data from the solar dehydrator's heating process were graphed against internal solar energy for both pretreatments, as shown in Figs. 10 and 11. The regression analysis results showed a remarkably significant linear relationship (r = 0.9213 and r = 0.9253, in order; P > 0.001). The regression equations with the best fit were as shown in Eqs. 45 and 46:

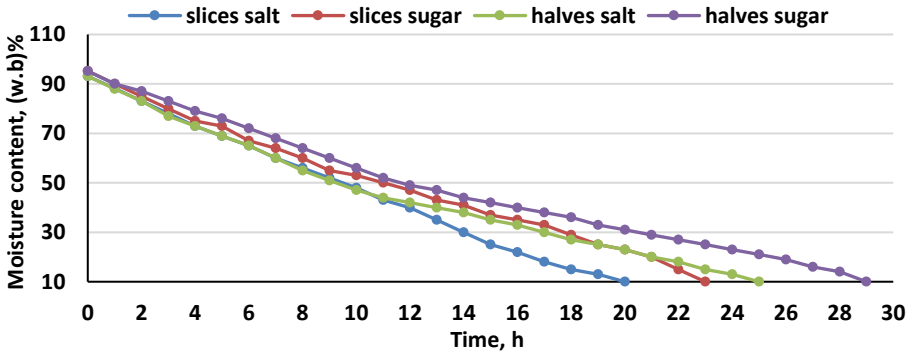

Fig. 9 – Variation of tomatoes moisture contents for salt and sugar treatments inside the lean-to solar dryer

$$Hp\ (salt) = 0.8428\ (q) \tag{45}$$

$$Hp\ (sugar) = 0.7118\ (q) \tag{46}$$

Regression analysis shows that 84.28% and 71.18% of solar energy were used for heating power in the tomato dehydrator system. The solar dehydrator lost the remaining solar energy (15.72% and 28.82%, respectively) through various modes of heat transfer (radiation, convection, conduction, and exhausted air) to the surroundings.

Useful heat gain and heat losses

During the experiment, the dryer's average heat gain ranged from 1350 to 1850 Wh per day. The quantity of heat that proved useful displayed variations over the experimental duration owing to the changes in weather. The reduction in the ambient air temperature (Tamb) led to a decrease in the useful heat gain because of the diminished temperature difference between the hot air inside the dryer and the air flowing from the collector to the dryer.

In the lean-to solar dryer, the average daily heat gain for evaporating moisture from tomatoes decreased from 60% to 5% at the beginning and end of the dehydration process. The remaining heat was lost through convection, conduction, and radiation. It is essential to acknowledge that the increase in temperature difference between the solar dryer's interior and the surrounding air increases heat losses.

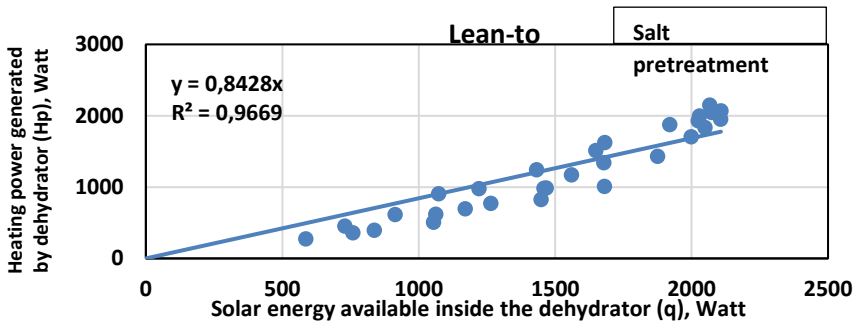

Fig. 10 – Heating energy generated by the lean-to solar dehydrator against solar energy inside the dehydrator for salt pretreatment

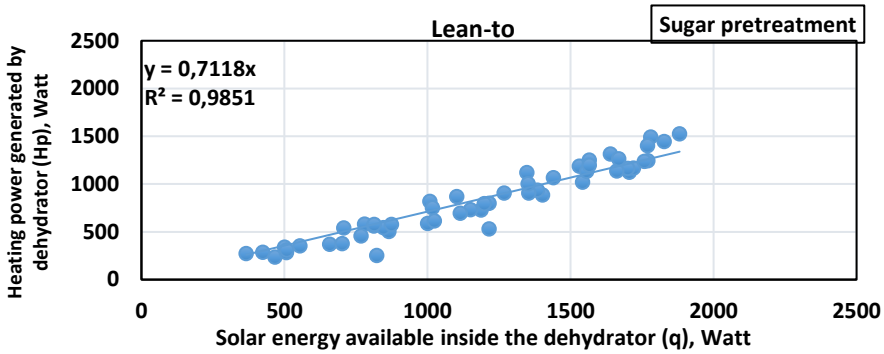

Fig. 11 – Heating energy generated by the lean-to solar dehydrator against solar energy inside the dehydrator for the sugar pretreatment

Assessing the relationship between solar energy and heating power is necessary to evaluate the solar dehydrator's thermal performance and overall efficiency. The solar dehydrator was found to provide an average diurnal solar energy of 54.939 kWh, while generating a heating power of 39.670 kWh for salt pretreatment during the 25-hour dehydrating process. Thus, the solar dehydrator attained an overall thermal efficiency of 76.2%. As a result, the exhausted dehydrating air lost about 23.8% of the heating power. The average daily total solar energy within the lean-to solar dehydrator and the generated heating power during the experimental period (29 hours) amounted to 59.375 kWh and 47.473 kWh, respectively. Consequently, the total thermal efficiency of the lean-to solar dehydrator reached 79.95%. As a result, the dehydrator experienced a loss of approximately 20.05% in heating power when the dehydrating air was discharged. The solar dryer exhibited minimal heat infiltration through the door and connections; hence, it was disregarded. During cloudy hours, the remaining usable energy produced by the PV module can be stored in the battery, along with the energy required for operating the DC fan. The solar energy inside the lean-to solar dehydrator (E_{in}), solar energy outside (E_{out}), the overall thermal efficiency (η_{th}), and the energy losses during each hour throughout the dehydrating process are summarized and presented in Table 2.

Overall thermal efficiency

The drying system was assessed, including energy analysis, energy efficiency, and time-dependent changes in energy loss. The drying system component's input, output, energy losses, and efficiency are illustrated in Figs. 12 and 13. The average overall efficiency for the salt and sugar pretreatment was 53.5% and 48.1%, respectively. The salt pretreatment was the best because of its short drying time of 25 hours. The presence of clouds, which caused solar radiation to scatter, decreased the efficiency of various components and input energy within the drying system. An increased disparity between output and input energy resulted in reduced efficiency. The collector's mean efficiency was 65.1% and 57.5% for the salt and sugar pretreatment, respectively. In contrast, the solar dryer's optimal mean efficiency has a comparable pattern to solar collectors. This result is associated explicitly with the drying time, whereby the salt experiment on slices exhibited the shortest period. The collector's efficiency was noted to be at its peak on the first day and displayed a continuous decline throughout the second, third, and fourth days. This can be because the drying rate initially started at a high value and gradually decreased over time until the end of the experiment.

Nonetheless, the sugar trial yielded the highest mean efficiency for the PV system. It could be because of the solar radiation incident on the PV panel throughout the experiment. Figs. 12 and 13 rely on the thermal analysis of the solar system, considering solar radiation and weather conditions during the experiment. These figures' energy inputs in (E_{in}) depend on the solar radiation during the experiment. The energy output (E_{out}) is the energy that exits each part of the drying system after use. The E_{loss} represents the disparity between E_{in} and E_{out} for the solar collector; the energy input (E_{in}) denotes the energy acquired from solar radiation, which progressively increases from morning until 1:00 p.m. and decreases until the day's ending. The energy output (E_{out}) refers to the energy expelled through the outlet after accounting for energy losses (E_{loss}) from the bottom, sides, and cover.

Table 2

The solar energy inside the lean-to solar dehydrator (E_{in}), solar energy outside (E_{out}), the overall thermal efficiency (η_{th}), and the energy losses during each hour throughout the dehydrating process

	Salt pretreatment				Sugar pretreatment			
Solar collector	E_{in}, Wh	E_{out}, Wh	E_{loss}, Wh	Efficiency, %	E_{in}, Wh	E_{out}, Wh	E_{loss}, Wh	Efficiency, %
	887.8	620.0	244.4	72.3	806.0	530.0	246.0	63.9
	757.8	581.1	260.0	62.7	644.0	256.0	283.0	56.0
	680.0	467.0	207.0	60.3	333.8	390.0	147.0	60.9
	-	-	-	-	348.0	405.0	161.0	49.3
Solar dryer								
	1725.0	315.0	1318.8	49.7	1725.0	144.0	1290.0	56.1
	1740.0	206.0	1695.0	49.7	1155.0	71.0	1015.0	53.7
	1531.0	32.4	1377.5	45.0	655.0	40.0	550.0	52.5
	-	-	-	-	817.9	49.0	573.0	51.5
PV panels								
	503.0	38.9	414.4	12.0	437.0	392.0	46.0	11.7
	444.0	51.0	378.0	12.5	395.0	372.0	47.1	13.5
	358.8	40.4	322.5	14.9	199.0	181.5	53.5	13.4
	-	-	-	-	221.0	215.0	55.7	17.9

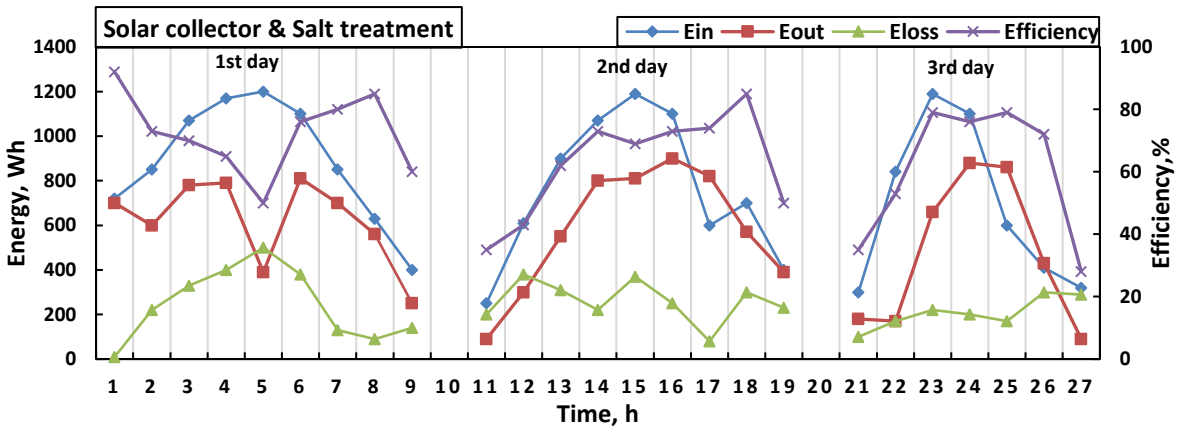

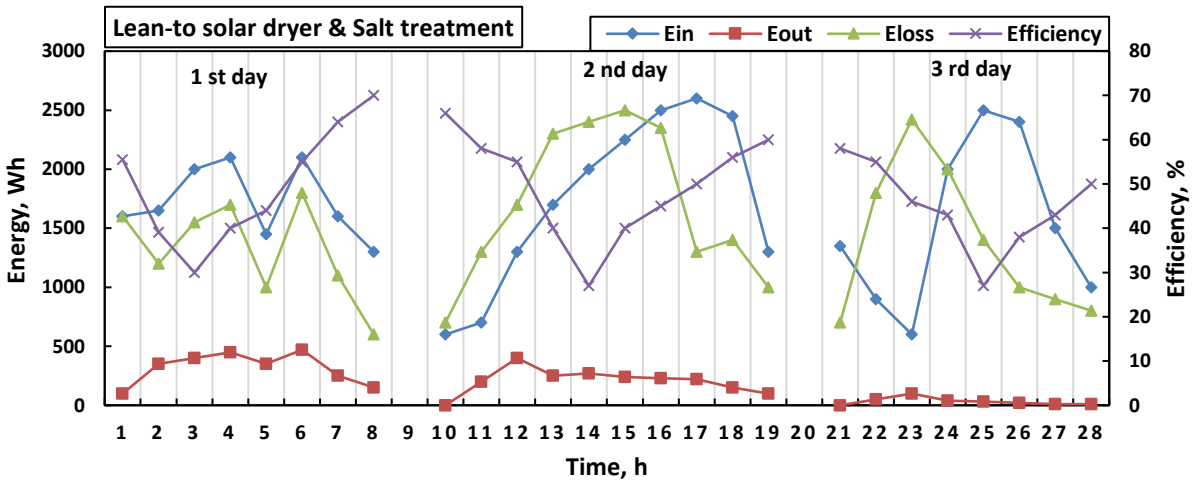

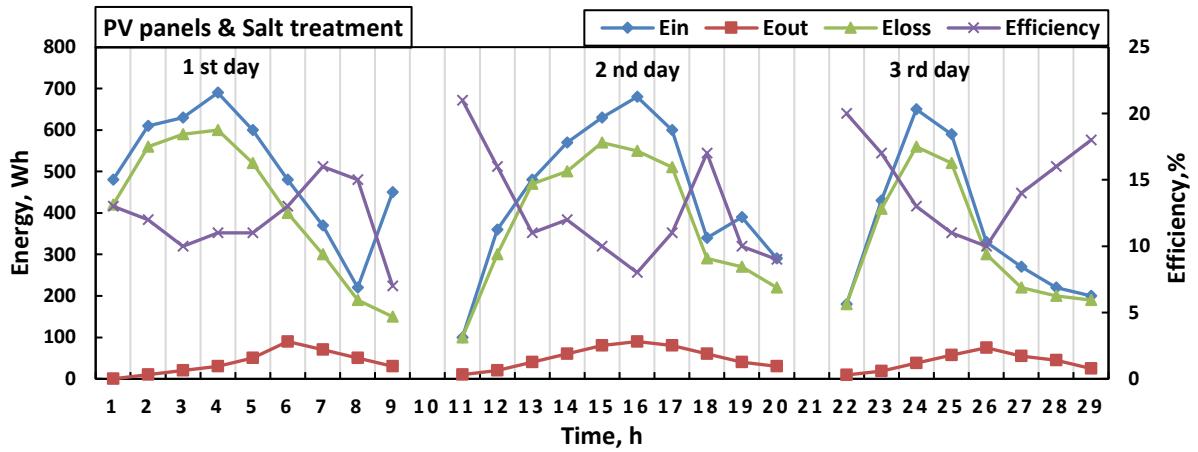

Fig. 12 – The calculated energy input (E_{in}), energy output (E_{out}), energy loss (E_{loss}), and efficiency for collector, dryer, and PV for salt treatment of slices and halves tomatoes

The E_{out} started with a small value, progressively escalating in response to the strength of solar radiation until reaching a maximum, followed by a gradual decline by day's end. The solar collector's efficiency has an inverse relationship with energy loss. The dryer's performance may vary based on weather conditions, as shown in Figs. 12 and 13. The E_{out} implies the energy released upon the evaporation of moisture from the tomatoes; beginning at a high level, it progressively decreases in correspondence with the moisture content until the solar drying process ends. The value was significantly higher on the initial day because of the high reduction in the tomato's moisture content. Afterward, a decrease was observed on the second day because of the tomato moisture content reduction, eventually reaching its lowest point on the third day when the moisture content became exceedingly low. PV panels had a behavior similar to solar collectors, but their efficiency trend differed regarding energy input and loss. Furthermore, it was varied based on the weather conditions. The useful energy is exploited to dry the tomatoes in the drying system by quickly lessening the tomato's moisture content to a safe level. Hence, the usefulness of solar energy diminished over time. The results demonstrated a progressive rise in E_{loss} with passaging drying time throughout each day until mid-day, after which it declined. Air temperature and moisture content are critical factors that significantly influence E_{loss}. Additionally, it was noted that E_{loss} initially exhibited a high value in these trials. The results revealed that energy efficiency exhibited higher on the first day than the last, which can be attributed to increased losses during the drying process. Additionally, the temperature variation led to an elevation in the E_{loss} resulting from radiation and convection heat exchange between the internal cover and other dryer elements. The significant temperature variation observed between the indoor and outdoor air of the dryer suggests that the chosen dryer design exhibited a high-efficiency level.

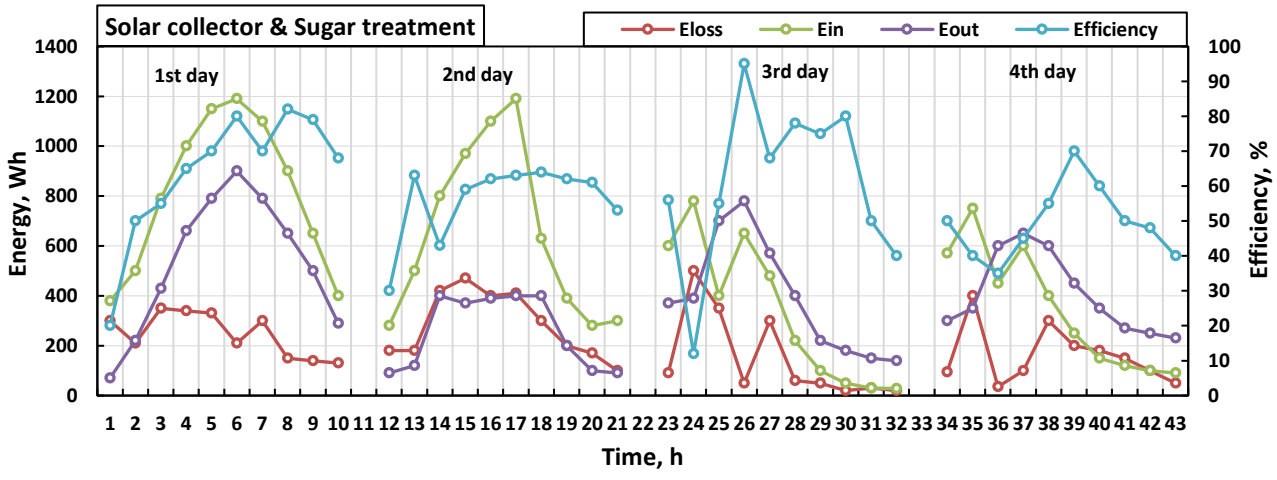

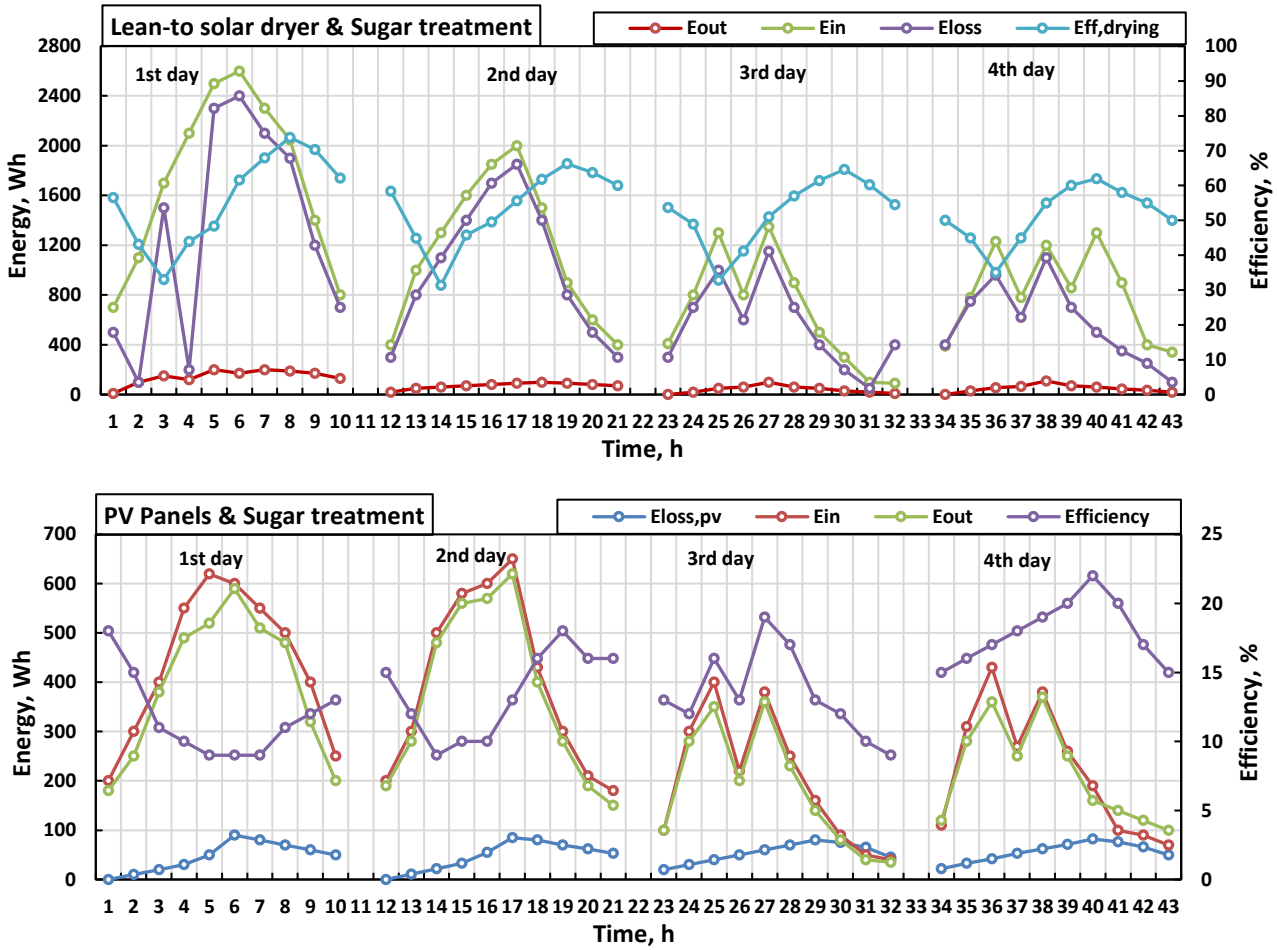

Fig. 13 – The calculated energy input (E_{in}), energy output (E_{out}), energy loss (E_{loss}), and efficiency for collector, dryer, and PV for sugar treatment of slices and halves tomatoes

CONCLUSIONS

The solar dryer (lean-to) was developed to optimize the absorption of solar radiation for efficient heat gain. The solar drying system's thermal efficiency was examined by investigating its mixed-mode forced convection. The moisture content was removed using solar-heated air with temperatures ranging from 40 to 60°C, air-relative humidity between 19 and 40%, and incident solar radiation ranging from 400 to 1200 W/m². As a result, the solar dehydrator utilized a suction blower to expel water vapor, enabling the transfer of sensible and latent heat during the evaporation process of water. Different pretreatments before drying were examined to detect the optimal treatment. Further, energy for various components of the lean-to-solar dryer was analyzed. The results showed that the dried tomatoes attained the state of equilibrium moisture content within the drying equipment for slices and halves (salt) after 20 and 25 hours, respectively. In contrast, sugar treatment was 23 and 29 h, respectively. The initial drying rate of tomato slices was higher than the halves. The tomato slices that underwent salt pretreatment and were dried in the dryer exhibited the shortest drying time compared with those that underwent sugar pretreatment. Tomato halves were dipped in sucrose solution (40%) and then dried in the dryer for 72 h, which had the longest drying period. Increasing the energy difference between input and output reduces efficiency. The highest level of mean efficiency for the PV system was observed on the fourth day during the sugar pretreatment phase (slices and halves of tomatoes). The average overall efficiencies for the salt and sugar pretreatments were 53.5% and 48.1%, respectively. The salt pretreatment was the optimal choice, resulting in the shortest drying time of 25 hours. The mean efficiency for the collector was 65.1 and 57.5% for the salt, and sugar pretreatment, respectively.

REFERENCES

[1] Abdellatif, S.M., El-Hadidi, Y.M., & Mohammed, E.M. (2015). Thermal performance analysis for solar collector air heater assisted solar modified-Quonset dryer. *Journal of Soil Sciences and Agricultural Engineering, Mansoura University 6*(10), 1217–1236. https://dx.doi.org/10.21608/jssae.2015.43796

[2] ASAE (1991). *Standard*s. American society of agricultural engineers, st. Joseph. Michigan.
[3] Azam, M.M., Eltawil, M.A., & Amer, B.M. (2020). Thermal analysis of PV system and solar collector integrated with greenhouse dryer for drying tomatoes. *Energy,* 212, 118764. https://doi.org/10.1016/j.energy.2020.118764
[4] Bergman, T.L., Lavine, A.S., Incropera, F.P., & DeWitt, D.P. (2011). *Introduction to heat transfer*. John Wiley & Sons.
[5] Cengel, A. (2003). *Heat transfer: A practical approach*. New York: McGraw-Hill.
[6] Dewanto, V., Wu, X., Adom, K.K., & Liu, R.H. (2002). Thermal processing enhances the nutritional value of tomatoes by increasing total antioxidant activity. *Journal of agricultural and food chemistry,* 50(10), 3010–3014. https://doi.org/10.1021/jf0115589
[7] Duffie, J. A., & Beckman, W.A. (2013). *Solar engineering of thermal processes*. New York, N.Y.: John Wiley and Sons. http://doi.org/10.1002/9781118671603
[8] Eltawil, M.A., Azam, M.M., & Alghannam, A.O. (2018). Energy analysis of hybrid solar tunnel dryer with PV system and solar collector for drying mint (MenthaViridis). *Journal of Cleaner Production* 181, 352–364. https://doi.org/10.1016/j.jclepro.2018.01.229
[9] Faostat (2018). *http://www.fao.org/faostat/ar/#data/QC*.
[10] FAO (2022). *Food and Agriculture Organization of the United Nations*. FAOSTAT Available at https://www.fao.org/faostat/en/#data/QCL, accessed on 04/03/2024.
[11] Hepbasli, A. (2008). A key review on exergetic analysis and assessment of renewable energy resources for a sustainable future. *Renew Sustain Energy Rev*., 12(3), 593–661. https://doi.org/10.1016/j.rser.2006.10.001
[12] Lakshmi, D.V.N., Muthukumar, P., Layek, A., & Nayak, P.K. (2019). Performance analyses of mixed mode forced convection solar dryer for drying of stevia leaves. *Solar Energy*, 188, 507–518. https://doi.org/10.1016/j.solener.2019.06.009
[13] Lewicki, P.P. (1998). Some remarks on rehydration of dried foods. *Journal of Food Engineering,* 36(1), 81–87. https://doi.org/10.1016/S0260-8774(98)00022-3
[14] Li, M. (2021). Research on color correction method of greenhouse tomato plant image based on high dynamic range imaging. *NMATEH - Agricultural Engineering,* 64(2), 393-402. https://doi.org/10.35633/inmateh-64-39
[15] Mohsenin, N.N., (2020). *Physical properties of plant and animal materials: v. 1: physical characteristics and mechanical properties*. Routledge.
[16] Mumba, J. (1996). Design and development of a solar grain dryer incorporating photovoltaic powered air circulation. *Energy Convers Manag*. 37(5), 615-621. https://doi.org/10.1016/0196-8904(95)00205-7
[17] Patil, R., & Gawande, R. (2016). A review on solar tunnel greenhouse drying system. *Renewable and sustainable energy reviews,* 56, 196–214. https://doi.org/10.1016/j.rser.2015.11.057
[18] Ramos, I.N., Brandao, T.R.S., & Silva, C.L.M. (2015). Simulation of solar drying of grapes using an integrated heat and mass transfer model. *Renewable Energy,* 81, 896–902. https://doi.org/10.1016/j.renene.2015.04.011
[19] Sahin, S., & Sumnu, S.G. (2005). *Physical properties of foods*. USA: Springer. https://hdl.handle.net/11511/70305
[20] Shahi, M.M.N., Sabetghadam, M., & Athari, M. (2016). The Effect of Osmotic and Ultrasound Pretreatment on Some Physicochemical Features of Avocado. *International Journal of Pharmaceutical Research & Allied Sciences,* 5(4), 121–131.
[21] Tiwari, S., & Tiwari, G.N. (2016). Exergoeconomic analysis of photovoltaic-thermal (PVT) mixed mode greenhouse solar dryer. *Energy,* 114, 155–164. https://doi.org/10.1016/j.energy.2016.07.132
[22] Usub, T., Lertsatitthanakorn, C., Poomsa-ad, N., Wiset, L., Yang, L., & Siriamornpun, S. (2008). Experimental performance of a solar tunnel dryer for drying silkworm pupae. *Biosystems Engineering,* 101(2), 209–216. https://doi.org/10.1016/j.biosystemseng.2008.06.011